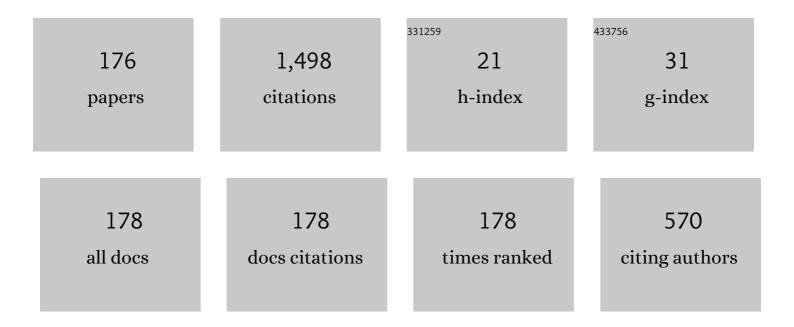
Innokenty I Novikov

List of Publications by Year in descending order

Source: https://exaly.com/author-pdf/8130368/publications.pdf Version: 2024-02-01



#	Article	IF	CITATIONS
1	High power temperature-insensitive 1.3 µm InAs/InGaAs/GaAs quantum dot lasers. Semiconductor Science and Technology, 2005, 20, 340-342.	1.0	150
2	MBE-grown metamorphic lasers for applications at telecom wavelengths. Journal of Crystal Growth, 2007, 301-302, 914-922.	0.7	51
3	High-power single mode (>1W) continuous wave operation of longitudinal photonic band crystal lasers with a narrow vertical beam divergence. Applied Physics Letters, 2008, 92, .	1.5	44
4	A 1.33 µm InAs/GaAs quantum dot laser with a 46 cm ^{â^'1} modal gain. Semiconductor Science and Technology, 2008, 23, 105004.	1.0	41
5	Vertical-Cavity Surface-Emitting Lasers Based on Submonolayer InGaAs Quantum Dots. IEEE Journal of Quantum Electronics, 2006, 42, 849-856.	1.0	40
6	High-performance 640-nm-range GaInP-AlGaInP lasers based on the longitudinal photonic bandgap crystal with narrow vertical beam divergence. IEEE Journal of Quantum Electronics, 2005, 41, 1341-1348.	1.0	35
7	6-mW Single-Mode High-Speed 1550-nm Wafer-Fused VCSELs for DWDM Application. IEEE Journal of Quantum Electronics, 2017, 53, 1-8.	1.0	33
8	High-power InAs/GaInAs/GaAs QD lasers grown in a multiwafer MBE production system. Journal of Crystal Growth, 2005, 278, 335-341.	0.7	31
9	Metamorphic 1.5 µm-range quantum dot lasers on a GaAs substrate. Semiconductor Science and Technology, 2006, 21, 691-696.	1.0	31
10	Heterostructures for quantum-cascade lasers of the wavelength range of 7–8 μm. Technical Physics Letters, 2017, 43, 666-669.	0.2	31
11	High-power singlemode CW operation of 1.5â€[micro sign]m-range quantum dot GaAs-based laser. Electronics Letters, 2005, 41, 478.	0.5	30
12	Wavelength-stabilized tilted cavity quantum dot laser. Semiconductor Science and Technology, 2004, 19, 1183-1188.	1.0	28
13	Effect of p-Doping of the Active Region on the Temperature Stability of InAsâ^•GaAs QD Lasers. Semiconductors, 2005, 39, 477.	0.2	28
14	Degradation-robust single mode continuous wave operation of 1.46μm metamorphic quantum dot lasers on GaAs substrate. Applied Physics Letters, 2006, 89, 041113.	1.5	28
15	High-Power Low-Beam Divergence Edge-Emitting Semiconductor Lasers with 1- and 2-D Photonic Bandgap Crystal Waveguide. IEEE Journal of Selected Topics in Quantum Electronics, 2008, 14, 1113-1122.	1.9	27
16	Single mode cw operation of 658nm AlGaInP lasers based on longitudinal photonic band gap crystal. Applied Physics Letters, 2006, 88, 231108.	1.5	24
17	Dual-Frequency Generation in Quantum Cascade Lasers of the 8-μm Spectral Range. Optics and Spectroscopy (English Translation of Optika I Spektroskopiya), 2018, 125, 402-404.	0.2	24
18	Tilted Wave Lasers: A Way to High Brightness Sources of Light. IEEE Journal of Quantum Electronics, 2011, 47, 1014-1027.	1.0	22

#	Article	IF	CITATIONS
19	Reliability performance of 25 Gbit s ^{â^'1} 850 nm vertical-cavity surface-emitting lasers. Semiconductor Science and Technology, 2013, 28, 065010.	1.0	22
20	Room-temperature operation of quantum cascade lasers at a wavelength of 5.8 î¼m. Semiconductors, 2016, 50, 1299-1303.	0.2	22
21	Progress on single mode VCSELs for data- and tele-communications. Proceedings of SPIE, 2012, , .	0.8	21
22	High-power (>1 W) room-temperature quantum-cascade lasers for the long-wavelength IR region. Quantum Electronics, 2020, 50, 141-142.	0.3	20
23	Room Temperature Lasing of Multi-Stage Quantum-Cascade Lasers at 8 μm Wavelength. Semiconductors, 2018, 52, 1082-1085.	0.2	18
24	Lasing of multiperiod quantum-cascade lasers in the spectral range of (5.6–5.8)-μm under current pumping. Semiconductors, 2015, 49, 1527-1530.	0.2	17
25	Room Temperature Lasing of Single-Mode Arched-Cavity Quantum-Cascade Lasers. Technical Physics Letters, 2019, 45, 398-400.	0.2	17
26	QD lasers: physics and applications. , 2005, , .		16
27	Ultrahigh gain and non-radiative recombination channels in 1.5 µm range metamorphic InAs–InGaAs quantum dot lasers on GaAs substrates. Semiconductor Science and Technology, 2005, 20, 33-37.	1.0	16
28	High-power high-brightness semiconductor lasers based on novel waveguide concepts. Proceedings of SPIE, 2010, , .	0.8	16
29	Heterostructures of Single-Wavelength and Dual-Wavelength Quantum-Cascade Lasers. Semiconductors, 2018, 52, 745-749.	0.2	16
30	High-Power Quantum-Cascade Lasers Emitting in the 8-μm Wavelength Range. Technical Physics Letters, 2019, 45, 735-738.	0.2	16
31	Narrow vertical beam divergence laser diode based on longitudinal photonic band crystal waveguide. Electronics Letters, 2003, 39, 1729.	O.5	15
32	Waferâ€fused 1300Ânm VCSELs with an active region based on superlattice. Electronics Letters, 2021, 57, 697-698.	0.5	15
33	High Power Single Mode 1300-nm Superlattice Based VCSEL: Impact of the Buried Tunnel Junction Diameter on Performance. IEEE Journal of Quantum Electronics, 2022, 58, 1-15.	1.0	15
34	Lasing in 9.6-μm Quantum Cascade Lasers. Technical Physics, 2018, 63, 1511-1515.	0.2	14
35	High power GalnPâ^•AlGalnP visible lasers (=646â€nm) with narrow circular shaped far-field pattern. Electronics Letters, 2005, 41, 741.	0.5	13
36	High power GaAsâ^•AlGaAs lasers (λâ^1⁄4850nm) with ultranarrow vertical beam divergence. Applied Physics Letters, 2006, 89, 231114.	1.5	13

#	Article	IF	CITATIONS
37	A high-power 975 nm tilted cavity laser with a 0.13 nm K ^{â^'1} thermal shift of the lasing wavelength. Semiconductor Science and Technology, 2007, 22, 1061-1065.	1.0	13
38	Low divergence edge-emitting laser with asymmetric waveguide based on one-dimensional photonic crystal. Physica Status Solidi C: Current Topics in Solid State Physics, 2005, 2, 919-922.	0.8	12
39	Anomalous dynamic characteristics of semiconductor quantum-dot lasers generating on two quantum states. Technical Physics Letters, 2007, 33, 4-7.	0.2	12
40	High-power one-, two-, and three-dimensional photonic crystal edge-emitting laser diodes for ultra-high brightness applications. Proceedings of SPIE, 2008, , .	0.8	12
41	Optical Gain in Laser Heterostructures with an Active Area Based on an InGaAs/InGaAlAs Superlattice. Optics and Spectroscopy (English Translation of Optika I Spektroskopiya), 2019, 127, 1053-1056.	0.2	12
42	Collective resonance and form factor of homogeneous broadening in semiconductors. Applied Physics Letters, 2000, 76, 2514-2516.	1.5	11
43	Temperature Dependence of the Effective Coefficient of Auger Recombination in 1.3 μm InAsâ^•GaAs QD Lasers. Semiconductors, 2005, 39, 481.	0.2	11
44	Turn-on Dynamics of Quantum Cascade Lasers with a Wavelength of 8100 nm at Room Temperature. Technical Physics, 2018, 63, 1656-1658.	0.2	11
45	Continuous-wave Lasing of Single-Mode Metamorphic Quantum Dot Lasers for the 1.5-μm Spectral Region. Semiconductors, 2005, 39, 1415.	0.2	10
46	Wavelength-stabilized tilted wave lasers with a narrow vertical beam divergence. Semiconductor Science and Technology, 2008, 23, 075043.	1.0	10
47	Temperature and current dependences of the lasing spectrum's width of quantum dot lasers. Semiconductors, 2009, 43, 1597-1601.	0.2	10
48	Temperature characteristics of low-threshold high-efficiency quantum-dot lasers with the emission wavelength from 1.25 to 1.29 µm. Semiconductors, 2003, 37, 1239-1242.	0.2	9
49	Longitudinal photonic bandgap crystal laser diodes with ultra-narrow vertical beam divergence. , 2006, , .		9
50	VCSELs based on arrays of sub-monolayer InGaAs quantum dots. Semiconductors, 2006, 40, 615-619.	0.2	9
51	20 Gbit/s error free transmission with ~850 nm GaAs-based vertical cavity surface emitting lasers (VCSELs) containing InAs-GaAs submonolayer quantum dot insertions. Proceedings of SPIE, 2009, , .	0.8	9
52	On the gain properties of "thin―elastically strained InGaAs/InGaAlAs quantum wells emitting in the near-infrared spectral region near 1550 nm. Semiconductors, 2016, 50, 1412-1415.	0.2	9
53	Analysis of the Internal Optical Losses of the Vertical-Cavity Surface-Emitting Laser of the Spectral Range of 1.55 µm Formed by a Plate Sintering Technique. Optics and Spectroscopy (English Translation) Tj ET	Qq10120.78	34394 rgBT
54	A Vertical-Cavity Surface-Emitting Laser for the 1.55-μm Spectral Range with Tunnel Junction Based on n++-InGaAs/p++-InGaAs/p++-InAlGaAs Layers. Technical Physics Letters, 2020, 46, 854-858.	0.2	9

#	Article	IF	CITATIONS
55	The Effect of a Saturable Absorber in Long-Wavelength Vertical-Cavity Surface-Emitting Lasers Fabricated by Wafer Fusion Technology. Technical Physics Letters, 2020, 46, 1257-1262.	0.2	9
56	Improved degradation stability of blue-green II-VI light-emitting diodes with excluded nitrogen-doped ZnSe-based layers. Semiconductors, 2001, 35, 1340-1344.	0.2	8
57	Single transverse mode 850â€nm GaAs/AlGaAs lasers with narrow beam divergence. Electronics Letters, 2006, 42, 1157.	0.5	8
58	High-power edge-emitting laser diode with narrow vertical beam divergence. Electronics Letters, 2011, 47, 1339.	0.5	8
59	Digital data transmission using electro-optically modulated vertical-cavity surface-emitting laser with saturable absorber. Applied Physics Letters, 2014, 104, .	1.5	8
60	Quantum-Cascade Lasers with a Distributed Bragg Reflector Formed by Ion-Beam Etching. Technical Physics Letters, 2020, 46, 312-315.	0.2	8
61	Heterostructures of Quantum-Cascade Laser for the Spectral Range of 4.6 μm for Obtaining a Continuous-Wave Lasing Mode. Technical Physics Letters, 2020, 46, 442-445.	0.2	8
62	Tilted cavity laser (Critical Review Lecture). , 2004, 5509, 61.		7
63	High-power wavelength stabilized 970nm tilted cavity laser with a 41.3dB side mode suppression ratio. Applied Physics Letters, 2007, 91, 241112.	1.5	7
64	Quantum dot insertions in VCSELs from 840 to 1300 nm: growth, characterization, and device performance. Proceedings of SPIE, 2009, , .	0.8	7
65	Optical properties of InGaAs/InGaAlAs quantum wells for the 1520–1580 nm spectral range. Semiconductors, 2016, 50, 1186-1190.	0.2	7
66	Optical Gain of 1550-nm Range Multiple-Quantum-Well Heterostructures and Limiting Modulation Frequencies of Vertical-Cavity Surface-Emitting Lasers Based on Them. Optics and Spectroscopy (English Translation of Optika I Spektroskopiya), 2018, 125, 238-242.	0.2	7
67	Broad-area InAsâ^•GaAs quantum dot lasers incorporating Intermixed passive waveguide. Electronics Letters, 2007, 43, 29.	0.5	6
68	The impact of thermal effects on the performance of vertical-cavity surface-emitting lasers based on sub-monolayer InGaAs quantum dots. Semiconductor Science and Technology, 2007, 22, 203-208.	1.0	6
69	A single-spatial-mode semiconductor laser based on InAs/InGaAs quantum dots with a diffraction filter of optical modes. Semiconductors, 2010, 44, 1357-1361.	0.2	6
70	Slow passage through thresholds in quantum dot lasers. Physical Review E, 2016, 94, 052208.	0.8	6
71	Continuous wave and modulation performance of 1550nm band wafer-fused VCSELs with MBE-grown InP-based active region and GaAs-based DBRs. Proceedings of SPIE, 2017, , .	0.8	6
72	High Temperature Laser Generation of Quantum-Cascade Lasers in the Spectral Region of 8 μm. Physics of the Solid State, 2018, 60, 2291-2294.	0.2	6

#	Article	IF	CITATIONS
73	Vertical-cavity surface-emitting lasers with intracavity contacts and a rhomboidal current aperture for compact atomic clocks. Quantum Electronics, 2019, 49, 187-190.	0.3	6
74	Influence of Output Optical Losses on the Dynamic Characteristics of 1.55-μm Wafer-Fused Vertical-Cavity Surface-Emitting Lasers. Semiconductors, 2019, 53, 1104-1109.	0.2	6
75	Spectral Characteristics of Half-Ring Quantum-Cascade Lasers. Optics and Spectroscopy (English) Tj ETQq1 1 0.7	'84314 rgE 0.2	BT/Overlock
76	10-W 4.6-μm quantum cascade lasers. Quantum Electronics, 2020, 50, 720-721.	0.3	6
77	Superradiance in semiconductors. Semiconductors, 1999, 33, 1309-1314.	0.2	5
78	High brilliance photonic band crystal lasers. , 2006, 6350, 22.		5
79	Edge-emitting InGaAs/GaAs laser with high temperature stability of wavelength and threshold current. Semiconductor Science and Technology, 2010, 25, 045003.	1.0	5
80	High-speed single-mode quantum dot and quantum well VCSELs. Proceedings of SPIE, 2011, , .	0.8	5
81	Dropout dynamics in pulsed quantum dot lasers due to mode jumping. Applied Physics Letters, 2015, 106, 261103.	1.5	5
82	1.55-μm-Range Vertical-Cavity Surface-Emitting Lasers, Manufactured by Wafer Fusion of Heterostructures Grown by Solid-Source Molecular-Beam Epitaxy. Semiconductors, 2020, 54, 1276-1283.	0.2	5
83	850 nm optical components for 25 Gb/s optical fiber data communication links over 100 m at 85ŰC. , 2011, , .		4
84	Influence of optical losses on the dynamic characteristics of linear arrays of near-infrared vertical-cavity surface-emitting lasers. Semiconductors, 2013, 47, 844-848.	0.2	4
85	Degradation-robust 850-nm vertical-cavity surface-emitting lasers for 25Gb/s optical data transmission. Semiconductors, 2014, 48, 77-82.	0.2	4
86	High-speed 1.3 -1.55 um InGaAs/InP PIN photodetector for microwave photonics. Journal of Physics: Conference Series, 2017, 917, 052029.	0.3	4
87	Growth and optical characterization of 7.5 μ4m quantum-cascade laser heterostructures grown by MBE. Journal of Physics: Conference Series, 2018, 1124, 041029.	0.3	4
88	On the Impact of Barrier-Layer Doping on the Photoluminescence Efficiency of InGaAlAs/InGaAs/InP Strained-Layer Heterostructures. Semiconductors, 2018, 52, 1156-1159.	0.2	4
89	Vertical-Cavity Surface-Emitting 1.55-μm Lasers Fabricated by Fusion. Technical Physics Letters, 2018, 44, 24-27.	0.2	4

#	Article	IF	CITATIONS
91	1300-nm wafer-fused VCSELs with InGaAs/InAlGaAs superlattice-based active region. , 2022, , .		4
92	Collective Resonance and Form-Factor of Homogeneous Broadening in Semiconductors. Japanese Journal of Applied Physics, 1999, 38, 4772-4774.	0.8	3
93	Mechanism of dicke superradiance in semiconductor heterostructures. Semiconductors, 2004, 38, 837-841.	0.2	3
94	Edge and surface-emitting tilted cavity lasers (Invited Paper). , 2005, , .		3
95	Modeling of photonic-crystal-based high-power high-brightness semiconductor lasers. , 2010, , .		3
96	Metamorphic distributed Bragg reflectors for the 1440–1600 nm spectral range: Epitaxy, formation, and regrowth of mesa structures. Semiconductors, 2015, 49, 1388-1392.	0.2	3
97	Optical characterization of mid-infrared range quantum-cascade laser structures grown by MBE. Journal of Physics: Conference Series, 2017, 917, 052019.	0.3	3
98	Spectral Shift of Quantum-Cascade Laser Emission under the Action of Control Voltage. Technical Physics Letters, 2019, 45, 1136-1139.	0.2	3
99	Optically pumped non-zero field magnetometric sensor for the magnetoencephalographic systems using intra-cavity contacted VCSELs with rhomboidal oxide current aperture. Journal of Physics: Conference Series, 2020, 1697, 012175.	0.3	3
100	Observation of Long Turn-On Delay in Pulsed Quantum Cascade Lasers. Journal of Lightwave Technology, 2022, 40, 2104-2110.	2.7	3
101	1.3 μm optically-pumped monolithic VCSEL based on GaAs with InGa(Al)As superlattice active region. Laser Physics Letters, 2022, 19, 075801.	0.6	3
102	Collective resonances and shape function for homogeneous broadening of the emission spectra of quantum-well semiconductor heterostructures. Semiconductors, 1999, 33, 779-781.	0.2	2
103	1.3-1.5 μm quantum dot lasers on foreign substrates: growth using defect reduction technique, high-power CW operation, and degradation resistance. , 2006, , .		2
104	Experimental study of temperature dependence of threshold characteristics in semiconductor VCSELs based on submonolayer InGaAs QDs. Semiconductors, 2006, 40, 1232-1236.	0.2	2
105	MBE-grown ultra-large aperture single-mode vertical-cavity surface-emitting laser with all-epitaxial filter section. Journal of Crystal Growth, 2007, 301-302, 945-950.	0.7	2
106	High-gain injection quantum-dot lasers operating at wavelengths above 1300 nm. Technical Physics Letters, 2008, 34, 1008-1010.	0.2	2
107	Single-Lobe Single-Wavelength Lasing in Ultrabroad-Area Vertical-Cavity Surface-Emitting Lasers Based on the Integrated Filter Concept. IEEE Journal of Quantum Electronics, 2008, 44, 724-731.	1.0	2
108	A temperature-stable semiconductor laser based on coupled waveguides. Semiconductors, 2011, 45, 550-556.	0.2	2

#	Article	IF	CITATIONS
109	Design concepts of monolithic metamorphic vertical-cavity surface-emitting lasers for the 1300–1550 nm spectral range. Semiconductors, 2015, 49, 1522-1526.	0.2	2
110	Optical properties of metamorphic GaAs/InAlGaAs/InGaAs heterostructures with InAs/InGaAs quantum wells, emitting light in the 1250–1400-nm spectral range. Semiconductors, 2016, 50, 612-615.	0.2	2
111	Lasing of metamorphic hybrid 1300nm spectral band VCSEL under optical pumping up to 120 ŰC. , 2017, , .		2
112	Optical properties of metamorphic hybrid heterostuctures for vertical-cavity surface-emitting lasers operating in the 1300-nm spectral range. Semiconductors, 2017, 51, 1127-1132.	0.2	2
113	The Influence of Cavity Design on the Linewidth of Near-IR Single-Mode Vertical-Cavity Surface-Emitting Lasers. Technical Physics Letters, 2018, 44, 28-31.	0.2	2
114	Quantum-Cascade Lasers with U-Shaped Resonator: Single Frequency Generation at Room Temperature. , 2019, , .		2
115	Generation of Frequency Combs by Quantum Cascade Lasers Emitting in the 8-μm Wavelength Range. Technical Physics Letters, 2019, 45, 1027-1030.	0.2	2
116	Effect of coherent population trapping in a compact microfabricated Cs gas cell pumped by intra-cavity contacted VCSELs with rhomboidal oxide current aperture. Journal of Physics: Conference Series, 2019, 1400, 077014.	0.3	2
117	Tunable single-frequency source based on a DFB laser array for the spectral region of 1.55 μm. Quantum Electronics, 2019, 49, 1158-1162.	0.3	2
118	Spectral Dynamics of Quantum Cascade Lasers Generating Frequency Combs in the Long-Wavelength Infrared Range. Technical Physics, 2020, 65, 1281-1284.	0.2	2
119	The Influence of the Parameters of a Short-Period InGaAs/InGaAlAs Superlattice on Photoluminescence Efficiency. Technical Physics Letters, 2020, 46, 1128-1131.	0.2	2
120	Design of the New Control System for Linac-200. Physics of Particles and Nuclei Letters, 2020, 17, 600-603.	0.1	2
121	Dynamics of Frequency Combs Generation by QCLs in 8 \hat{l} 4 m Wavelength Range. , 2020, , .		2
122	Surface Emitting Quantum-Cascade Ring Laser. Semiconductors, 2021, 55, 591.	0.2	2
123	Degradation of NSe-Free Blue-Green ZnSe-Based Light Emitting Diodes with Superlattice Miniband Hole Transport. Physica Status Solidi (B): Basic Research, 2002, 229, 1019-1023.	0.7	1
124	Generation of superradiation in quantum dot nanoheterostructures. Semiconductors, 2008, 42, 714-719.	0.2	1
125	Efficient electro-optic semiconductor medium based on type-II heterostructures. Semiconductors, 2013, 47, 1528-1538.	0.2	1

126 The effect of slow passage in the pulse-pumped quantum dot laser. , 2014, , .

1

#	Article	IF	CITATIONS
127	MBE growth and characterization of InAlAs/InGaAs 9 μm range quantum cascade laser. Journal of Physics: Conference Series, 2017, 917, 052016.	0.3	1
128	Phosphorus-free mode-locked semiconductor laser with emission wavelength 1550 nm. Journal of Physics: Conference Series, 2017, 917, 052021.	0.3	1
129	Dual-band generation around 8 μm by quantum cascade lasers in wide temperature range. Journal of Physics: Conference Series, 2018, 1135, 012073.	0.3	1
130	Quantum-cascade lasers of mid-IR spectral range: epitaxy, diagnostics and device characteristics. EPJ Web of Conferences, 2018, 195, 04001.	0.1	1
131	Quantum-cascade lasers in the 7-8 μm spectral range with full top metallization. Journal of Physics: Conference Series, 2018, 993, 012031.	0.3	1
132	Mode-Locked Lasers with "Thin―Quantum Wells in 1.55 μ m Spectral Range. Technical Physics Letters, 2018, 44, 174-177.	0.2	1
133	Temperature Dependence of the Parameters of 1.55-μm Semiconductor Lasers with Thin Quantum Wells Based on Phosphorus-Free Heterostructures. Technical Physics Letters, 2019, 45, 549-552.	0.2	1
134	Spontaneous Emission and Lasing of a Two-Wavelength Quantum-Cascade Laser. Semiconductors, 2019, 53, 345-349.	0.2	1
135	High-power λ = 8 µm quantum-cascade lasers at room temperature. Journal of Physics: Conference Series, 2019, 1400, 066048.	0.3	1
136	High-coupling distributed feedback lasers for the 1.55 μm spectral region. Quantum Electronics, 2019, 49, 801-803.	0.3	1
137	Study of the Spectra of Arched-Cavity Quantum-Cascade Lasers. Optics and Spectroscopy (English) Tj ETQq1 1	0.784314	rgBT /Overl <mark>oc</mark>
138	Influence of the doping type on the temperature dependencies of the photoluminescence efficiency of InGaAlAs/InGaAs/InP heterostructures. Journal of Luminescence, 2021, 239, 118393.	1.5	1
139	Quantum-Cascade Ring Resonator Laser with 7–8 μm Wavelength and Surface Radiation Output. Semiconductors, 2020, 54, 1816-1819.	0.2	1
140	A Study of the Spatial-Emission Characteristics of Quantum-Cascade Lasers for the 8-μm Spectral Range. Technical Physics Letters, 2020, 46, 1152-1155.	0.2	1
141	The Technique for QCLs Heating Dynamics Mesurements. , 2020, , .		1
142	Characterization of lasing regimes of 1.3  µm vertical-cavity surface-emitting lasers based on a short-period InGaAs/InGaAlAs superlattice. Journal of Optical Technology (A Translation of) Tj ETQq0 0 0 rgBT /C	verbaek 10) Tf150 137 Td
143	Treatment of inhomogeneous radiation broadening in quantum dot heterostructures described within the framework of the superradiation model. Technical Physics Letters, 2000, 26, 259-261.	0.2	Ο

Waveguide InGaAsP/InP photodetectors for low-power autocorrelation measurements at 1.55 Âμm.
0.2 0

#	Article	IF	CITATIONS
145	Electroluminescence of injection lasers based on vertically coupled quantum dots near the lasing threshold. Semiconductors, 2003, 37, 112-114.	0.2	Ο
146	Two-photon absorption in InGaAsP waveguides. , 2003, , .		0
147	Peculiarities of electroluminescence of quantum dot laser heterostructures. , 2003, 5036, 67.		0
148	Superradiance as a transition phase from spontaneous to stimulated emission in low-dimensional semiconductor heterostructures. , 2003, , .		0
149	Electroluminescent studies of emission characteristics of InGaAsN/GaAs injection lasers in a wide temperature range. Semiconductors, 2004, 38, 727-731.	0.2	Ο
150	Competition Of Different Recombination Channels In Metamorphic 1.5 μm Range Quantum Dot Lasers On GaAs Substrate. AIP Conference Proceedings, 2007, , .	0.3	0
151	Tilted cavity concept for the high-power wavelength stabilized diode lasers. , 2008, , .		Ο
152	Quantum dot semiconductor lasers of the 1.3 μm wavelength range with high temperature stability of the lasing wavelength (0.2 nm/K). Semiconductors, 2009, 43, 680-684.	0.2	0
153	Dynamical interplay between ground and excited states in quantum dot laser. , 2014, , .		Ο
154	Evidence of negative electrorefraction in type-II GaAs/GaAlAs short-period superlattice. Semiconductor Science and Technology, 2015, 30, 115013.	1.0	0
155	Impact of the carrier relaxation paths on two-state operation in quantum dot lasers. , 2015, , .		Ο
156	1550â€nm mode-locked semiconductor lasers for all-optical analog-to-digital conversion. AIP Conference Proceedings, 2017, , .	0.3	0
157	The concept for realization of quantum-cascade lasers emitting at 7.5 μm wavelength. Journal of Physics: Conference Series, 2017, 929, 012082.	0.3	0
158	Semiconductor light sources for near- and mid-infrared spectral ranges. Journal of Physics: Conference Series, 2017, 917, 022003.	0.3	0
159	Molecular-beam epitaxy of 7-8 μm range quantum-cascade laser heterostructures. Journal of Physics: Conference Series, 2017, 929, 012081.	0.3	0
160	Quantum-cascade lasers of 8-9 μm spectral range. , 2018, , .		0
161	Effect of barrier doping on photoluminescence of 1550 nm range multi quantum well heterostructures , 2018, , .		0
162	A heterostructure for resonant-cavity GaAs p-i-n photodiode with 840-860 nm wavelength. Journal of Physics: Conference Series, 2019, 1236, 012071.	0.3	0

#	Article	IF	CITATIONS
163	Temperature performance of InGaAs/InGaAlAsTemperature performance of InGaAs/InGaAlAs laser diodes with δ-doping active region. Journal of Physics: Conference Series, 2019, 1410, 012104.	0.3	0
164	Observation of the increase in turn-on delay of quantum cascade lasers under pulsed electrical pumping with finite rise time. Journal of Physics: Conference Series, 2020, 1697, 012062.	0.3	0
165	Investigation of optical and structural properties of three-dimensional InGaPAs islands formed by substitution of elements of the fifth group. Journal of Physics: Conference Series, 2020, 1697, 012106.	0.3	0
166	Turn-on delay in the mid-infrared quantum-cascade lasers: experiment and numerical simulations. , 2021, , .		0
167	Optical Properties of Three-Dimensional InGaP(As) Islands Formed by Substitution of Fifth-Group Elements. Optics and Spectroscopy (English Translation of Optika I Spektroskopiya), 2021, 129, 256-260.	0.2	0
168	High-Power (>13 W) Quantum-Cascade Lasers for Long Wavelength Infrared Range. , 2020, , .		0
169	Vertical cavity surface emitting laser of 1.55 \hat{l} /4m spectral range, manufactured by molecular beam epitaxy and wafer fusion technique. Journal of Physics: Conference Series, 2020, 1697, 012178.	0.3	0
170	Effect of saturable absorber in 1.5 μm wafer-fused vertical cavity surface-emitting lasers. Journal of Physics: Conference Series, 2020, 1697, 012167.	0.3	0
171	1.55 µm range edge-emitting laser diodes based on InGaAs/InGaAlAs superlattice and InGaAs quantum wells. Journal of Physics: Conference Series, 2020, 1695, 012072.	0.3	0
172	Turn-on Delay of Quantum Cascade Lasers under Pulsed Pumping with Non-zero Rise-time. , 2020, , .		0
173	High Power Quantum-Cascade Lasers for 8 \hat{l} $^{1}\!4$ m Spectral Region. , 2020, , .		0
174	Intensity noise characteristics of intracavity contacted VCSELs with rhomboidal oxide current aperture for the magnetometric sensor with Cs ¹³³ vapor cell used in magnetoencephalography. Journal of Physics: Conference Series, 2021, 2103, 012182.	0.3	0
175	Investigation of the zinc diffusion process into epitaxial layers of indium phosphide and indium-gallium arsenide grown by molecular beam epitaxy. Journal of Optical Technology (A) Tj ETQq1 1 0.7843	14 og 14)ve d ock 10
176	Quantum-Cascade Laser with Radiation Emission through a Textured Layer. Semiconductors, 2022, 56, 1-4.	0.2	0